Nanotechnology

Immobilization hemin into metal-organic frameworks as electrochemical biosensor for 2,4,6-trichlorophenol

To cite this article before publication: Ting Zhang *et al* 2017 *Nanotechnology* in press https://doi.org/10.1088/1361-6528/aaa26e

Immobilization hemin into metal-organic frameworks as electrochemical biosensor for 2,4,6-trichlorophenol

Ting Zhang[1,2], Lu Wang[1], Congwei Gao[1], Chaoyue Zhao[1], Yang Wang[1] and Jianmin Wang[2]

[1] School of Chemistry and Chemical Engineering, Yangzhou University, Yangzhou 225002, China.

[2] State Key Laboratory of Trauma, Burns and Combined Injury, Institute of Surgery Research, Daping Hospital, Third Military Medical University, Chongqing 400042, China.

E-mail: wangyzu@126.com and jmwang@tmmu.edu.cn

ABSTRACT

Hemin immobilized into copper-based metal-organic framework were successfully prepared and used as new electrode materials for sensitive electrochemical biosensing. X-ray diffraction patterns, Fourier transform infrared spectra, scanning electron microscope, UV-vis absorption spectroscopy, and cyclic voltammetry were used to characterize the resultant composites. Due to the interaction between the copper atom groups and hemin, the constrained environment in Cu-MOF-74 acts as a matrix to avoid the dimerization of enzyme molecule and retain its biological activity. The hemin/Cu-MOF composites demonstrated enhanced electrocatalytical activity and high stability towards the oxidation of 2,4,6-trichlorophenol. Under the optimum experimental conditions, the sensor shows a wide linear relationship over the range of 0.01 to 9 μmol L^{-1} with a detection limit (3σ) of 0.005 μmol L^{-1}. The relative standard deviations were 4.6% and 3.5% for 5 repeated measurements of 0.5 and 5 μmol L^{-1} 2,4,6-trichlorophenol, respectively. The detection platforms for 2,4,6-trichlorophenol developed here not only indicated that the hemin/Cu-MOF-74 possess intrinsic biological reactivity but also conduct further work toward the application of enzyme-containing metal-organic frameworks in electrochemical biosensors.

Keywords: Metal-organic frameworks, hemin, 2,4,6-trichlorophenol, electrochemical biosensor

1. Introduction

2,4,6-trichlorophenol (2,4,6-TCP) is commonly used in industry and agricultural chemicals. Due to the presence of chlorine atom and aryl structure, this compound has been considered a high environmental pollutant due to their possibly carcinogenic to humans [1, 2]. The no-effect concentration in aquatic environment established by the US Environmental Protection Agency is 0.097 mg/L [3]. Therefore, for the environment protection and human health purposes, a reliable and sensitive detection method for analysis of this compound is of particular significance, which should give a detection limit lower than the no-effect concentration as well as a suitable linear range to cover the actual concentration of 2,4,6-TCP in real samples.

So far, several methods using capillary electrophoresis [4], gas chromatography/liquid chromatography with different detector [5-7] are often used as official or no official methods for the quantitative of trace 2,4,6-TCP because of their highly efficient separations. However, all these procedures usually suffer from disadvantages such as tedious pretreatment procedure, time consumption and high cost. In comparison with the above methods, electrochemical technologies possess many advantages due to their good selectivity, low cost, high sensitivity, on-site determination, and have been reported for the detection of diverse chemical and biological species [8-10]. However, the use of enzymes as electrode materials for biosensors face sorts of challenges such as low operational stability, and cumbersome reusability [11, 12]. Hence, to our knowledge, limited number of such studies was reported. At this point, the immobilization of enzyme molecules into various supports including graphene [13], carbon nanotube [14], and montmorillonite clay [15] has been an efficient way to keep their catalytic activity.

Metal organic frameworks (MOFs), assembled with metal ions and organic linkers, have been recognized as type of highly porous materials. The outstanding physical and chemical properties of MOFs have attracted much attention as they contribute to their applications toward in many fields such as gas storage and separation as well as catalysis [16-18]. In addition, more efforts have been made to fabricate MOFs as a novel matrix for enzyme immobilization due to the unique

three-dimensional structure and high contact surface area [19-21], which can effectively prevent the dimerization of enzyme molecule. The enzyme-containing MOFs hybrid material showed preferable peroxidase-like activity than the free enzyme molecule in aqueous solution. For example, Ma et al. demonstrated the successful immobilization of the myoglobin into mesoporous MOFs host matrix, which exhibited excellent size-selective and catalytic bioactivities toward the oxidation of two organic substrates [22]. Wu et al. prepared multiple enzyme-containing metal-organic frameworks. It is found that the immobilization of enzymes in these metal-organic frameworks can improve the enzyme performance in ability, stability, and activity [23].

In this work, we developed copper-based metal-organic framework as efficient matrices of hemin immobilization for the building-up of electrochemical biosensor. 2,4,6-TCP was used as a model analyte and the associated high biocatalytic activity is revealed. The stepwise fabrication procedure and the detection mechanism of the enzyme-containing MOFs based electrochemical biosensor are shown in Scheme 1. Parameters that affect the analytical performance were systematically investigated prior to its determination with differential pulse voltammetry. The method was used for 2,4,6-TCP determination in environmental water samples and satisfactory results were obtained.

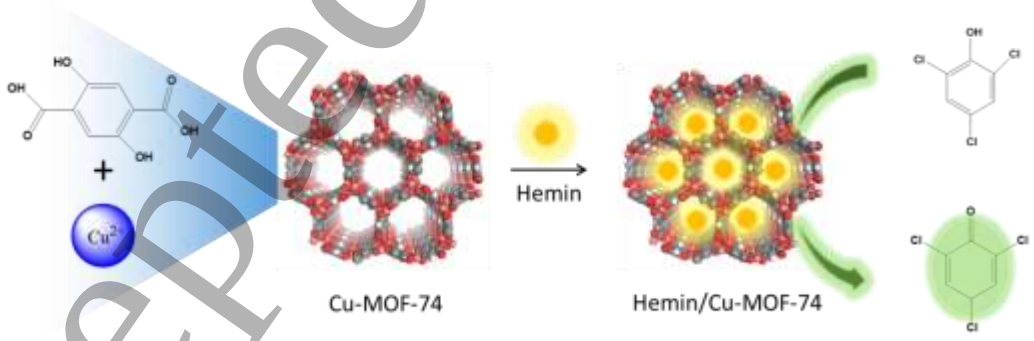

Scheme 1. The preparation of hemin/Cu-MOF-74 composites and the electrochemical mechanism for the detection of 2,4,6-TCP.

2. Experimental section

2.1. Reagents and materials

2,4,6-trichlorophenol (2,4,6-TCP), anhydrous ethanol, 2,5-dihydroxyterephthalic acid (H_2dhtp), *N,N*-dimethylformamide (DMF), trihydrated copper nitrate(II), and hemin were purchased from Sinopharm Chemical Reagent Co., Ltd. (Shanghai, China). Phosphate-buffered solution (PBS, 0.1 mol L^{-1}, pH 4.0-9.0) was prepared by using Na_2HPO_4 and NaH_2PO_4. Double deionized water used all through the experiments was obtained from Milli-Q water purification system (Millipore, Bdfedford, MA, USA). All other materials were used as received.

2.2. Apparatus

Electrochemical experiments were performed on a CHI660A electrochemical workstation (Chenhua Instrument, Shanghai, China) with a three-electrode system, which contains an Ag/AgCl reference electrode, a platinum wire counter electrode and a hemin/MOF-74 modified glassy carbon electrode (GCE) as working electrode. Powder X-ray diffraction (XRD) analysis was performed with a D8 Advance X-ray diffractometer (Bruker Co., Germany). Fourier-transform infrared spectroscopy (FTIR) spectra were measured with a Cary 610/670 infrared microspectrometer (Varian, America). The scanning electron micrograph (SEM) images were obtained with the S-4800 microscope (Hitachi, Japan). High-resolution transmission electron micrographs (HRTEM) were observed by using a FEI Tecnai G2 F30 S-TWIN field-emission transmission electron microscopy (USA). UV-Vis spectra were measured by UV-2550 spectro-photometer supplied by Shimadzu Co. (Japan).

2.3. Synthesis of Cu-MOF-74

Cu-MOF-74 was synthesized according to a previously reported method [24]: a mixture of 2.2 g 2,5-dihydroxyterephthalic acid and 5.9 g trihydrated copper nitrate(II) were added to a mixture of 20 mL DMF and 1 mL 2-propanoland, and heated to 80 ˚C for 18 h in an oven. The reddish needle-shaped crystals collected were then filtered, and washed with DMF and methanol. Finally, the crystals were dried at 150 ˚C for 5 h and stored under inert atmosphere before use.

2.4. Synthesis of hemin/Cu-MOF-74

To overcome the low aqueous solubility, a 20 g mL^{-1} hemin was prepared by dissolving 2.2g hemin in a 10 mL water and 15 mL methanol cosolvent system. hemin/Cu-MOF-74 was prepared by adding 5 mg of Cu-MOF-74 into 20 mL above hemin solution, and stirred for 6 h. The synthesized hemin/Cu-MOF-74 was centrifuged and washed with corresponding cosolvent, and dried at 80 ˚C for 5 h.

2.5. Preparation of modified electrode

The bare GCE was polished to a mirror-like surface with 0.03 μm alumina slurry and rinsed with ethanol and double deionized water for 10 min, and dried in nitrogen stream. After rinsing, 1.0 mg hemin/Cu-MOF-74 was dispersed into 1 mL DMF by sonication. 5 μL hemin/Cu-MOF-74 homogeneous solutions were coated on the surface of GCE and leave it for 24 h until the solvent was dried. Finally 5 mL 0.5% nafion solution was put on the hemin/Cu-MOF-74/GCE surface, and dried under room temperature. The obtained hemin/Cu-MOF-74/GCE was stored in refrigerator at 4 ˚C before use.

3. Results and discussion

3.1. Characterization of hemin/Cu-MOF-74

As shown in figure 1, preservation of the Cu-MOF-74 framework during the immobilization was confirmed by powder X-ray diffraction, which indicated the presence of characteristic peaks of Cu-MOF-74. The presence of the hemin was not detected in the XRD pattern of the hybrids, probably due to the weak signal of hemin compared to the MOF. Differences in the relative intensities of Cu-MOF-74 peaks after the immobilization can be explained by the decrease in the crystallinity.

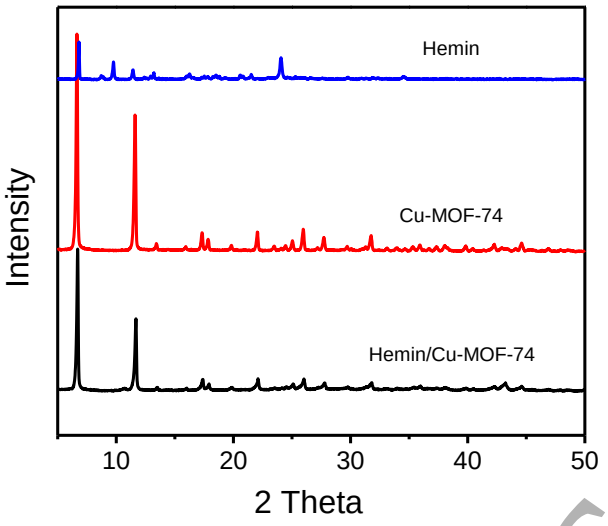

Figure 1. Powder X-ray diffraction patterns of hemin, Cu-MOF-74 and hemin/Cu-MOF-74.

The successful anchoring of hemin has been confirmed by FTIR studies (Figure 2). The Cu-MOF-74 spectra display several absorption peaks in the 600-1700 cm^{-1} range, which were attributed to the vibrational modes of the organic entities. The characteristic peaks in case of Cu-MOF-74 at 1425 and 1556 cm^{-1} were ascribed to the stretching vibration of the carboxylates present in the organic ligands [25]. As for hemin/Cu-MOF-74, the weak peak at 1717 cm^{-1} was ascribed to C=O stretching vibration, this was smaller than the peak at 1701 cm^{-1} in the curve of hemin due to the formation of the metal (Cu) carboxylate [26].

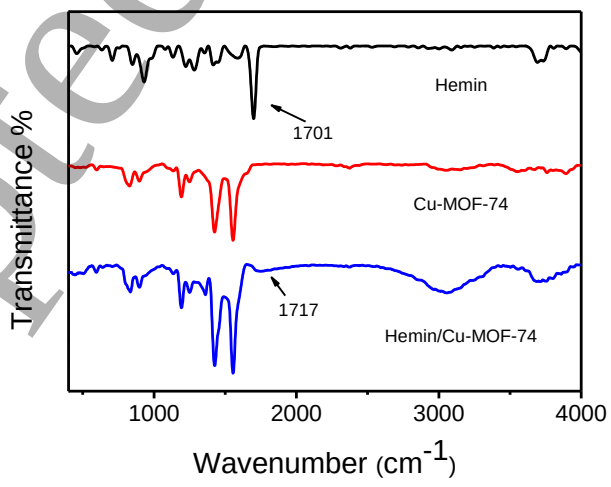

Figure 2. FTIR transmission spectra of hemin, Cu-MOF-74 and hemin/Cu-MOF-74.

The SEM images of the prepared composites revealed agglomerated needle-shaped crystals (figure. 3). After the Cu-MOF-74 was treated with the solution containing hemin, a large amount of hemin was clearly observed on the hemin/Cu-MOF-74 surface. Simultaneously, the energy dispersive X-ray spectroscopy (EDS) data revealed that Cu and Fe metal sites coexisted in the hemin-containing Cu-MOF-74 composites (figure S1), displaying the uniform distribution of hemin within the matrix. As hemin is a natural metalloporphyrin compound which contains a ferric iron ion with a chloride ligand. The EDS results demonstrate that hemin was immobilized in Cu-MOF-74 successfully.

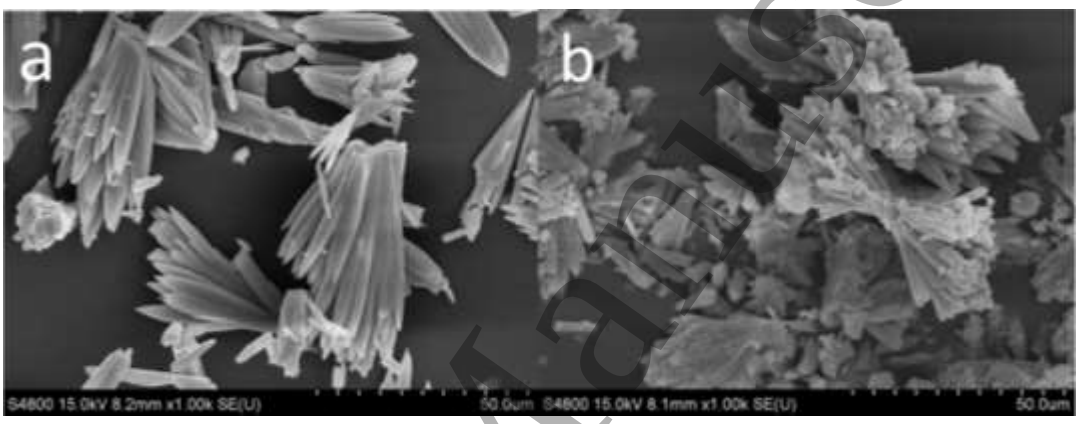

Figure 3. SEM images of Cu-MOF-74 (a) and hemin/Cu-MOF-74 (b).

As illustrated in figure 4, the UV-Vis absorption of free hemin showed a Soret peak at 383nm along with a shoulder at 371 nm, and the Cu-MOF-74 composites showed no adsorption. After immobilization of hemin into Cu-MOF-74, the Soret band of hemin shifted from 383nm to 396 nm, presumably due to the formation of covalent bonds between the copper atom groups on Cu-MOF-74 and carboxyl groups on hemin [27].

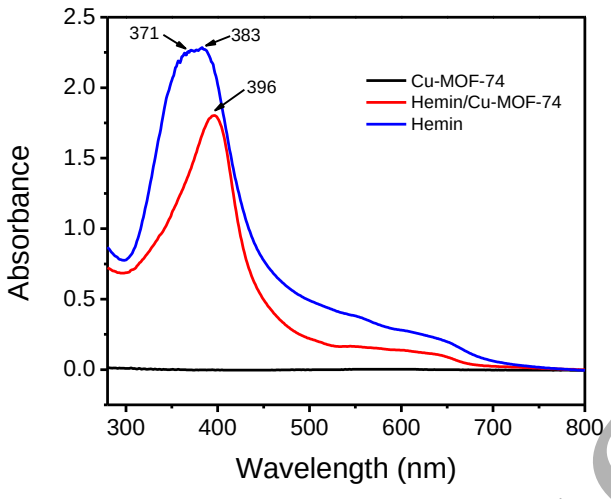

Figure 4. UV-Vis spectra of hemin, Cu-MOF-74, and hemin/Cu-MOF-74 in pH 7.0. phosphate buffer solution.

To demonstrate the peroxidase-like activity of the hemin/Cu-MOF-74, a classic chromogenic substrate TMB was adopted in the presence of H_2O_2. As shown in Fig. S2 in supporting information, there is no color change in TMB-H_2O_2 reaction system without a catalyst, and the Cu-MOF-74-TMB-H_2O_2 system also showed no color change in the same conditions. Conversely, the hemin/Cu-MOF-74-TMB-H_2O_2 system produced a deep blue color, suggesting that hemin/Cu-MOF-74 composites possess an intrinsic peroxidase mimic activity.

3.2. Electrocatalytic behavior of 2,4,6-TCP at the hemin/Cu-MOF-74/GCE

Figure 5 showed the cyclic voltammograms of 0.5 μmol L^{-1} 2,4,6-TCP at GCE, Cu-MOF-74/GCE, and hemin/Cu-MOF-74/GCE in 0.1 mol L^{-1} PBS (pH 7.0). The oxidation of 2,4,6-TCP at these electrodes is completely irreversible. The oxidation current intensity of 2,4,6-TCP on Cu-MOF-74/GCE was higher than that at GCE, which is assigned to the good conductivity and the high specific area of Cu-MOF-74 composites. When hemin was immobilized in the Cu-MOF-74, the current intensity at hemin/Cu-MOF-74/GCE was higher than those at other composites, probably owing to the synergistic effect produced by hemin and Cu-MOF-74. The reason for the improved performance may be contributed from the following properties: (I) Cu-MOF-74 consists of metal ions and organic ligands, which can adsorb more 2,4,6-TCP onto the electrode surface through π–π stacking interactions. (II)

Cu-MOF-74 possesses high surface areas, favoring high enzyme loading. (III) The possible interaction between enzyme and metal ions in Cu-MOF-74 increased the catalytic activity of hemin. Furthermore, the oxidation potential obtained at hemin/Cu-MOF-74/GCE (0.48 V) was lower than that at Cu-MOF-74/GCE (0.53 V) and GCE (0.66 V), indicating that the effect of coexisting species could be reduced.

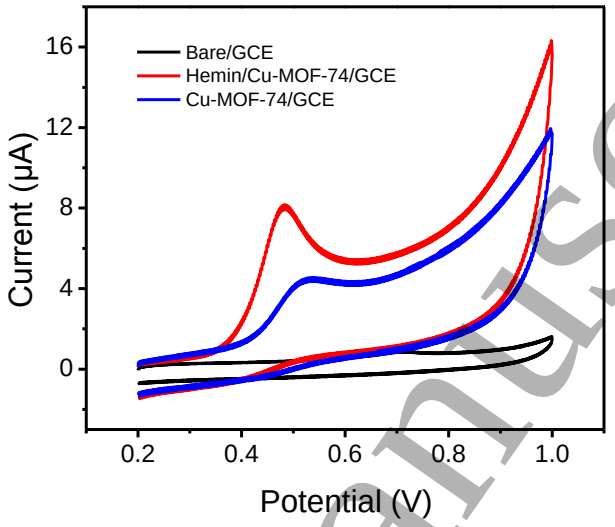

Figure 5. Cyclic voltammograms of 2,4,6-TCP at the bare GCE and GCEs modified with Cu-MOF-74, and hemin/Cu-MOF-74 in 0.1 mol L^{-1} PBS (pH=7.0).

Figure S3 showed the effect of the scan rate on the current intensity of 2,4,6-TCP at hemin/Cu-MOF-74/GCE over the range of 150 – 500 mVs^{-1}. With increasing scan rate, the current intensity was improved gradually. As shown in figure S3 inset, the oxidation peak current increased linearly with the square root of scan rate and can be expressed as: I_{pa} (lA) = 1.95 $v^{1/2}$ + 21.6 (mV s^{-1}) (R^2 = 0.991), which indicated that the diffusion-controlled played an important role in the electrode reaction.

The influence of pH on the current intensity of the hemin/Cu-MOF-74/GCE was studied (figure S4), and the current intensity increased with the pH value up to 7.0 and then decreased at higher pH values. Hence, a 0.1 mol L^{-1} PBS at pH 7.0 was selected as supporting electrolyte, considering the sensitivity of 2,4,6-TCP determination for all experiments. Moreover, the dependence of the oxidation peak potential (Epa) on pH values was also investigated. The oxidation peak potential of 2,4,6-TCP at Cu-MOF-74/GCE shifted more negative as pH value gradually increasing from 4.0 to

8.0 (figure S5), revealing that protons participate in the electrode reaction.

Accumulation can enhance the electrochemical response by improving the amount of 2,4,6-TCP absorbed on the electrode surface, therefore, the effects of accumulation conditions were examined (figure S6). The oxidation peak current was observed to increase gradually within the first 200 s and then increased much slightly, suggesting that the saturated adsorption of 2,4,6-TCP at the electrode surface occurred. Consequently, 200 s was employed to improve sensitivity and analysis frequency of the method. When the accumulation potential was investigated in the range from 0.2 to 0.8 V (figure S7), oxidation current reaches a maximum at the accumulation potential of 0.6 V. Thus, 0.6 V was used in all voltammetric determinations.

3.3. Interference experiment

Selectivity is an important factor in the performance of an electrochemical sensor, and different phenolic substrates such as nitrophenols, methylphenols and chlorophenols were individually evaluated. The tolerable concentration was defined as the current deviations caused by interference not exceeding ± 5.0%. It was found that 50-fold 2-nitrophenol (3.3%), 4-nitrophenol (4.1%), 2,4,6-nitrophenol (3.6%) did not show interference. 50-fold 2,3-methylphenol (6.1%), 2,4-methylphenol (5.7%) cause a slight interference. However, 2-fold 2-chlorophenol (9.2%), 3-chlorophenol (8.7%), 4-chlorophenol (8.9%), 2,3-dichlorophenol (9.5%), 2,4-dichlorophenol (9.3%), 2,5-dichlorophenol (8.8%) and 2,6-dichlorophenol (8.7%) had an obvious influence on the current intensity of 2,4,6-TCP, probably due to their the co-adsorption or similar peak potentials or at the hemin/Cu-MOF-74 electrode. Moreover, the effect of other foreign species was shown in the supporting information.

3.4. Analytical performance

Under the optimized experimental conditions, the differential pulse voltammograms of different concentrations of 2,4,6-TCP was displayed in figure 6. The peak current (Ip) increases linearly with the concentration of 2,4,6-TCP in the range from 0.01 to 9 μmol L^{-1} (figure 6). Two linear ranges were obtained in the ranges of 0.01−1.0 and 1.0−9.0 μmol L^{-1}, giving the following linear regressions: I_{pa} (μA) = 13.26C (μmol L^{-1}) + 0.03 (R^2 =0.996) and I_{pa} (μA) = 3.28C (μmol L^{-1}) + 1.74 (R^2 =0.998). The limit

of detection was found to be 0.005 μmol L^{-1} according to the signal-to-noise ratio of 3. The relative standard deviations of 4.6% and 3.5% for 5 measurements of 0.5 and 5 μmol L^{-1} of 2,4,6-TCP suggested that hemin/Cu-MOF-74/GCE had good repeatability. The analytical performance of the fabricated electrochemical sensor was compared with the other methods and the results were shown in Table 1. It is notable that the detection limit of this sensor is superior in some cases, as compared to the previously reported electrode materials for 2,4,6-TCP detection [28-32] and the max no-effect concentration of TCP defined by the US Environmental Protection Agency. It was also found that the prepared hemin/Cu-MOF-74/GCE could be used at least 6 cycles in the buffer solution without any decrease in voltammetric response compared with free hemin. The high sensitivity and stability can be attributed to the three-dimension porous structures in the Cu-MOF-74 matrix, which offer the biocompatible microenvironment to enhance the enzyme loading, and maintain the activity of the enzyme, in turn improve reaction efficiency. Although the disadvantages of this work were that the synthetic process of Cu-MOF-74 is relatively complicated and the morphology of Cu-MOF-74 is easily affected by the experimental conditions, the desirable analytical features of electrochemical biosensor combination with the immobilized enzyme system are especially suitable for on-situ detection trace levels of 2,4,6-TCP over other methods.

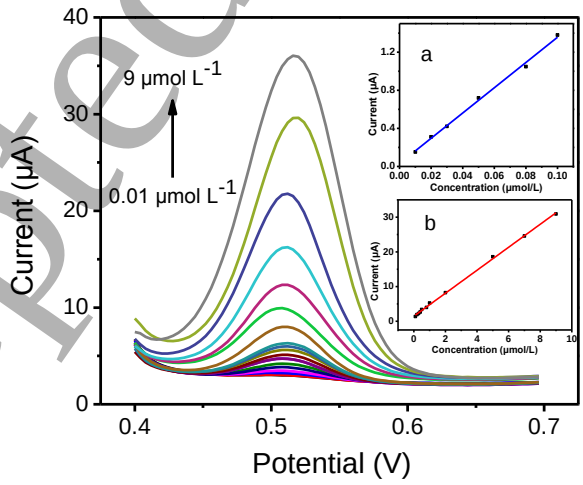

Figure 6. Differential pulse voltammograms at hemin/Cu-MOF-74/GCE in the presence of 0.01, 0.02, 0.03, 0.05, 0.08, 0.1, 0.2, 0.3, 0.4, 0.5, 0.8, 1, 2, 5, 7 and 9 μmol L^{-1} of 2,4,6-TCP. The insets show the plot of the peak currents as a function of

2,4,6-TCP concentrations in the range 0.01-1.0 (a), and 1.0-9.0 μmol L^{-1} (b), respectively.

Table 1. Comparison of the analytical performance with different electrode materials for the determination of 2,4,6-TCP

Detection method	Detection limit (μmol L^{-1})	Linear range (μmol L^{-1})	Ref.
CS@Ag@GO/GCE	0.0097	0.03-35	[28]
PPD-choroperoxidase/CPE	0.1	0.1-1	[29]
BCP/erGO/GCE	0.005	0.05-130	[30]
Imprinted microgel/CNT/SPE	25	-	[31]
HS-β-CD/AuNPs/SAM/ITO	0.001	0.003-0.028	[32]
Hemin/Cu-MOF-74/GCE	0.005	0.01-9	This work

CS：carbon sphere；GO：graphene oxide；PPD：poly(o-phenylendiamine)；CPE：carbon paste electrode；BCP: bromocresol purple; erGO: electrochemically reduced graphene oxide; CNT: carbon nanotubes; SPE: screen-printed electrode; CD: cyclodextrin; SAM: self-assembled monolayers; ITO: indium tin oxide.

3.5. Real sample analysis

The practical applicability the developed procedure was employed for the quantitative determination of 2,4,6-TCP in three environmental water samples. All the samples using the standard addition method undergo three parallel measurements. Before determination, the water sample was filtered with a 0.2 μm Millipore membrane. Each sample was determined directly or with an appropriate dilution to draw the 2,4,6-TCP concentration within the linear range. 50 μL sample solution was then transferred to a three-electrode cell and dissolved with 10 mL 0.1 mol · L^{-1} PBS (pH 7.0). The potential of preconcentration of 2,4,6-TCP was 0.6 V with a preconcentration time of 200 s. After 30 s equilibration time, the voltammogram in differential pulse mode was recorded with an anodic scan (potential range: 0.4 - 0.7 V; increment: 4 mV;

amplitude: 50 mV; pulse width: 0.2 s; sampling width: 0.02 s; pulse period: 0.5 s). The analytical results are shown in Table 2, and the recoveries of the 2,4,6-TCP in all samples were in the range of 98.0 - 104.0% with the RSDs less than 5%. The results demonstrate that the present method have good accuracy and could be used for the determination of 2,4,6-TCP.

Table 2. Determination of 2,4,6-TCP in water samples using hemin/Cu-MOF-74/GCE

Sample	Spiked (μmol L^{-1})	Found (μmol L^{-1})	Recovery (%)	RSD (%)
River water	0.05	0.05	100.0	4.23
	0.50	0.49	98.0	3.82
	5.00	5.10	102.0	3.11
Lake water	0.05	0.05	100.0	4.38
	0.50	0.52	104.0	3.41
	5.00	4.98	99.6	4.20
Tap water	0.05	0.05	100.0	4.15
	0.50	0.51	102.0	3.35
	5.00	4.96	99.2	3.39

4. Conclusions

In this work, we reported a simple method for the preparation of hemin-containing Cu-MOF-74 composite. The structural rigidity and confinement of the MOF can prevent the proteolysis and chelating of the embedded enzyme molecules and then enhance the stability of enzymes in aqueous medium. It was found that the application of the hemin/Cu-MOF-74 modified electrode as a novel electrochemical sensor has an excellent catalytic perfromance for 2,4,6-TCP oxidation in terms of high sensitivity, selectivity, and stability. The current intensity of 2,4,6-TCP was significantly

improved and the oxidation potential was also decreased. These features of hemin/Cu-MOF-74 composite make it promising for developing reliable 2,4,6-TCP biosensors. The parameters affecting the electrochemical process were investigated in detail. The new materials/strategy may create a new platform to enhance the performance of enzymes and offer wide applications in the fields of environmental monitoring and clinical diagnostics.

Acknowledgements

This work was supported by the National Natural Science Foundation of China (21205103, 21275124), Jiangsu Provincial Nature Foundation of China (BK2012258), Young and Middle-aged Academic Leaders Foundation of Yangzhou University, Top-notch Academic Programs Project of Jiangsu Higher Education Institutions (TAPP), and a project funded by the Priority Academic Program Development of Jiangsu Higher Education Institutions (PAPD).

References

[1] Yu GH, Wu MJ, Wei GR, Luo YH, Ran W, Wang BR, Zhang JC, and Shen QR 2012 Binding of organic ligands with Al(III) in dissolved organic matter from soil: implications for soil organic carbon storage *Environ. Sci. Technol.* 46 6102-6109.

[2] Tan IAW, Ahmad AL, and Hameed BH 2009 Adsorption isotherms, kinetics, thermodynamics and desorption studies of 2,4,6-trichlorophenol on oil palm empty fruit bunch-based activated carbon *J. Hazard. Mater.* 164 473-482.

[3] Jin XW, Zha JM, Xu YP, Giesy JP, Richardson KL, and Wang ZJ 2012 Derivation of predicted no effect concentrations (PNEC) for 2,4,6-trichlorophenol based on Chinese resident species *Chemosphere* 86 17-23.

[4] Muna GW, Quaiserová-Mocko V, and Swain GM 2005 Chlorinated phenol

analysis using off-line solid-phase extraction and capillary electrophoresis coupled with amperometric detection and a boron-doped diamond microelectrode *Anal. Chem.* 77 6542-6548.

[5] Feng QZ, Zhao LX, and Lin JM 2009 Molecularly imprinted polymer as micro-solid phase extraction combined with high performance liquid chromatography to determine phenolic compounds in environmental water samples *Anal. Chim. Acta.* 650 70-76.

[6] Campillo N, Peñalver R, and Hernández-Córdoba M 2006 Evaluation of solid-phase microextraction conditions for the determination of chlorophenols in honey samples using gas chromatography *J. Chromatogr. A* 1125 31-37.

[7] Ho TT, Chen CY, Li ZG, Yang TCC, and Lee MR 2012 Determination of chlorophenols in landfill leachate using headspace sampling with ionic liquid-coated solid-phase microextraction fibers combined with gas chromatography–mass spectrometry *Anal. Chim. Acta.* 712 72-77.

[8] Ciszewski A, and Milczarek G 1999 Polyeugenol-modified platinum electrode for selective detection of dopamine in the presence of ascorbic acid *Anal. Chem.* 71 1055-1061.

[9] Wei H, Sun JJ, Xie Y, Lin CG, Wang YM, Yin WH, and Chen GN 2007 Enhanced electrochemical performance at screen-printed carbon electrodes by a new pretreating procedure *Anal. Chim. Acta.* 588 297-303.

[10] Zhao HY, Ji XP, Wang BB, Wang N, Li XR, Ni RX, and Ren JJ 2015 An ultra-sensitive acetylcholinesterase biosensor based on reduced graphene oxide-Au nanoparticles-β-cyclodextrin/prussian blue-chitosan nanocomposites for organophosphorus pesticides detection *Biosens. Bioelectron.* 65 23-30.

[11] Mehta J, Bhardwaj N, Bhardwaj SK, Kim KH, and Deep A 2016 Recent advances in enzyme immobilization techniques: metal-organic frameworks as novel

substrates *Coordin. Chem. Rev.* 322 30-40.

[12] Huang Q, Huang QG, Pinto RA, Griebenow K, Schweitzer-Stenner R, and Weber WJ 2005 Inactivation of horseradish peroxidase by phenoxyl radical attack *J. Am. Chem. Soc.* 127 1431-1437.

[13] Guo YJ, Deng L, Li J, Guo SJ, Wang E, and Dong SJ 2011 Hemin-graphene hybrid nanosheets with intrinsic peroxidase-like activity for label-free colorimetric detection of single-nucleotide polymorphism *ACS Nano* 5 1282-1290.

[14] Zhang YF, Xu CL, and Li BX 2013 Self-assembly of hemin on carbon nanotube as highly active peroxidase mimetic and its application for biosensing *RSC Adv.* 3 6044-6050.

[15] Xiong J, Hang C, Gao J, Guo Y, and Gu C 2014 A novel biomimetic catalyst templated by montmorillonite clay for degradation of 2,4,6-trichlorophenol *Chem. Eng. J.* 254 276-282.

[16] Zou C, and Wu CD 2012 Functional porphyrinic metal-organic frameworks: crystal engineering and applications *Dalton Trans.* 41 3879-3888.

[17] Zhao M, Ou S, and Wu CD 2014 Porous metal–organic frameworks for heterogeneous biomimetic catalysis *Accounts. Chem. Res.* 47 1199-1207.

[18] Bromberg L, Su X, and Hatton TA 2013 Aldehyde self-condensation catalysis by aluminum aminoterephthalate metal–organic frameworks modified with aluminum isopropoxide *Chem. Mater.* 25 1636-1642.

[19] Lykourinou V, Chen Y, Wang XS, Meng L, Hoang T, Ming LJ, Musselman RL, and Ma SQ 2011 Immobilization of MP-11 into a mesoporous metal–organic framework, MP-11@mesoMOF: a new platform for enzymatic catalysis *J. Am. Chem. Soc.* 133 10382-10385.

[20] Xie SB, Ye JW, Yuan YL, Chai YQ, and Yuan R 2015 A multifunctional

hemin@metal-organic framework and its application to construct an electrochemical aptasensor for thrombin detection *Nanoscale* 7 18232-18238.

[21] Hou C, Wang Y, Ding QH, Jiang L, Li M, Zhu WW, Pan D, Zhu H, and Liu MZ 2015 Facile synthesis of enzyme-embedded magnetic metal-organic frameworks as a reusable mimic multi-enzyme system: mimetic peroxidase properties and colorimetric sensor *Nanoscale* 7 18770-18779.

[22] Chen Y, Lykourinou V, Hoang T, Ming LJ, and Ma SQ 2012 Size-selective biocatalysis of myoglobin immobilized into a mesoporous metal–organic framework with hierarchical pore sizes *Inorg. Chem.* 51 9156-9158.

[23] Wu XL, Ge J, Yang C, Hou M, and Liu Z 2015 Facile synthesis of multiple enzyme-containing metal-organic frameworks in a biomolecule-friendly environment *Chem. Commun.* 51 13408-13411.

[24] Calleja G, Sanz R, Orcajo G, Briones D, Leo P, and Martínez F 2014 Copper-based MOF-74 material as effective acid catalyst in friedel-crafts acylation of anisole *Catal. Today* 227 130-137.

[25] Adhikari AK, and Lin KS 2014 Synthesis, fine structural characterization, and CO_2 adsorption capacity of metal organic frameworks-74 *J. Nanosci. Nanotechnol.* 14 2709-2717.

[26] He J, Yang H, Zhang YY, Yu J, Miao LF, Song YH, and Wang L 2016 Smart nanocomposites of Cu-hemin metal-organic frameworks for electrochemical glucose biosensing *Sci. Rep.* 6 36637.

[27] Wang QG, Yang ZM, Zhang XQ, Xiao XD, Chang CK, and Xu B 2007 A supramolecular-hydrogel-encapsulated hemin as an artificial enzyme to mimic peroxidase *Angew. Chem. Int. Ed.* 46 4285-4289.

[28] Gan T, Lv Z, Sun JY, Shi ZX, and Liu YM 2016 Preparation of graphene

oxide-wrapped carbon sphere@silver spheres for high performance chlorinated phenols sensor *J. Hazard. Mater.* 302 188-197.

[29] Díaz-Díaz G, Blanco-López MC, Lobo-Castañón MJ, Miranda-Ordieres AJ, and Tuñón-Blanco P 2009 Chloroperoxidase modified electrode for amperometric determination of 2,4,6-trichlorophenol *Electroanalysis* 21 1348-1353.

[30] Zhu XL, Liu JG, Zhang ZS, Lu N, Yuan X, and Wu DM 2015 Green synthesis of a bromocresol purple/graphene composite and its application in electrochemical determination of 2,4,6-trichlorophenol *Anal. Methods* 7 3178-3184.

[31] Díaz-Díaz G, Blanco-López MC, Lobo-Castañón MJ, Miranda-Ordieres AJ, and Tuñón-Blanco P 2011 Preparation and characterization of a molecularly imprinted microgel for electrochemical sensing of 2,4,6-trichlorophenol *Electroanalysis* 23 201-208.

[32] Zheng XL, Liu S, Hua XX, Xia FQ, Tian D, and Zhou CL 2015 Highly sensitive detection of 2,4,6-trichlorophenol based on HS-β-cyclodextrin/gold nanoparticles composites modified indium tin oxide electrode *Electrochim. Acta.* 167 372-378.